Synergistic Dual-Plasticizer Engineering of Gel Polymer Electrolytes for Accelerated Zn^{2+} Transport and Stable Zinc Deposition

Sreshtha Ganguly[1], Dilip Bennada[1], Amrit Choudhury[1], Sreeraj Puravankara[1*]

[1]School of Energy Science and Engineering, Indian Institute of Technology Kharagpur, Kharagpur, West Bengal 721302, India

*Email: sreeraj@iitkgp.ac.in

Phone: +91(0)3222 260801

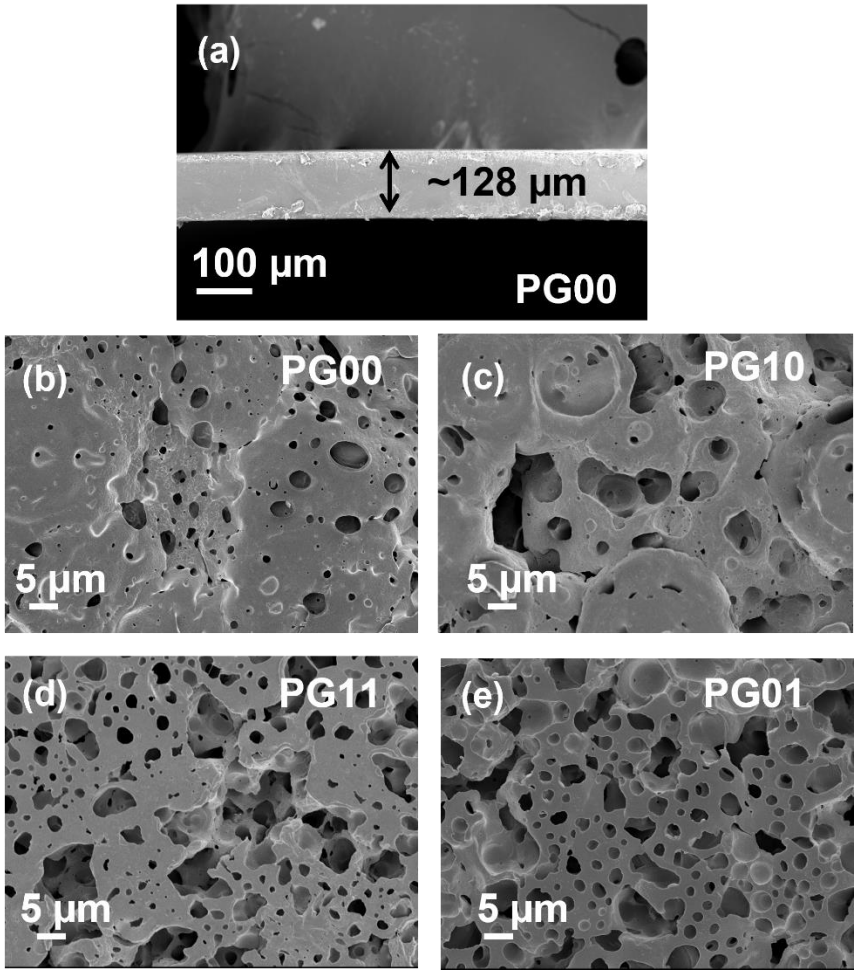

Figure S1. Morphological characterization of the gel polymer electrolyte membranes. (a) Cross-sectional SEM image of the PG00 membrane showing a thickness of approximately 128 μm; (b–e) Surface SEM images of the pristine PG00, PG10, PG11, and PG01 membranes, respectively.

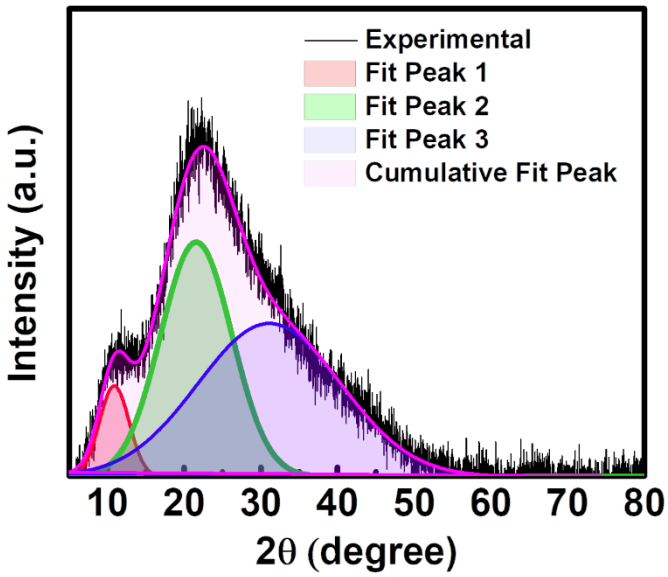

Figure S2. Representative peak deconvolution of the XRD pattern used for crystallinity analysis of the GPE membranes.

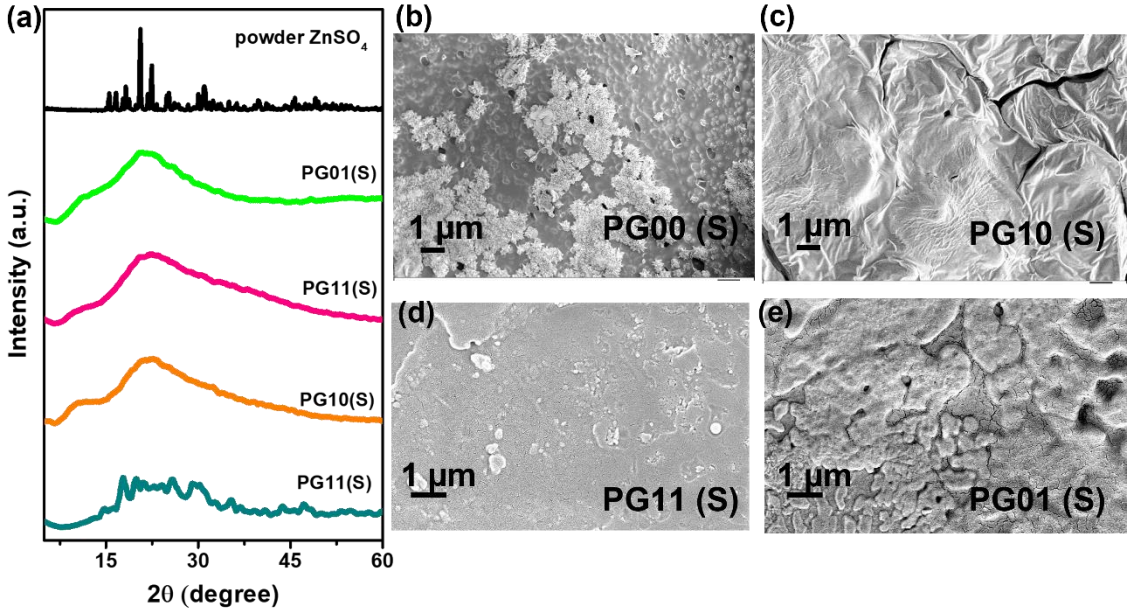

Figure S3. Structural and morphological characterization of $ZnSO_4$-soaked GPE membranes after drying. (a) XRD patterns of the dried $ZnSO_4$-soaked PG00, PG10, PG11, and PG01 membranes, together with pristine $ZnSO_4$ powder; (b–e) Surface SEM images of the corresponding dried $ZnSO_4$-soaked PG00, PG10, PG11, and PG01 membranes, respectively.

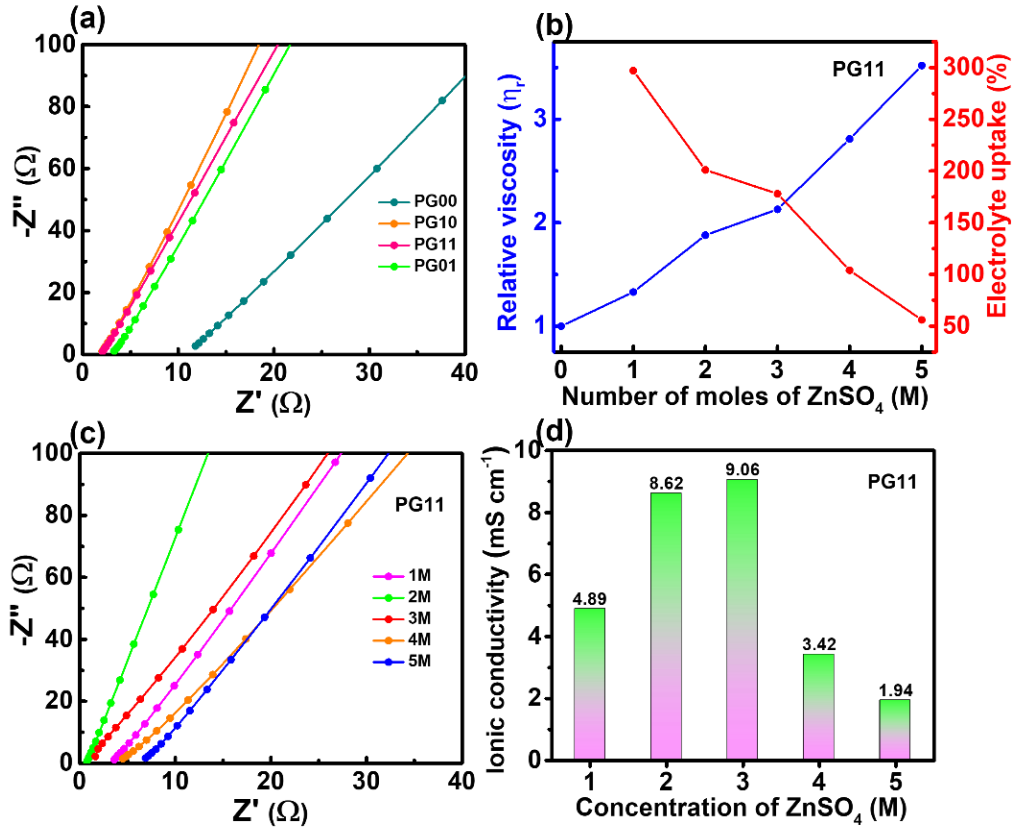

Figure S4. Electrochemical characterization and electrolyte concentration optimization of the GPEs. (a) Nyquist plots used for determining the ionic conductivity of PG00, PG10, PG11, and PG01; (b) Variation of the relative viscosity of $ZnSO_4$ solution and electrolyte uptake of the optimized PG11 membrane as a function of $ZnSO_4$ concentration; (c) Nyquist plots of the PG11 membrane soaked in $ZnSO_4$ electrolytes of different concentrations (1–5 M). (d) Ionic conductivity of the PG11 membrane as a function of $ZnSO_4$ concentration.

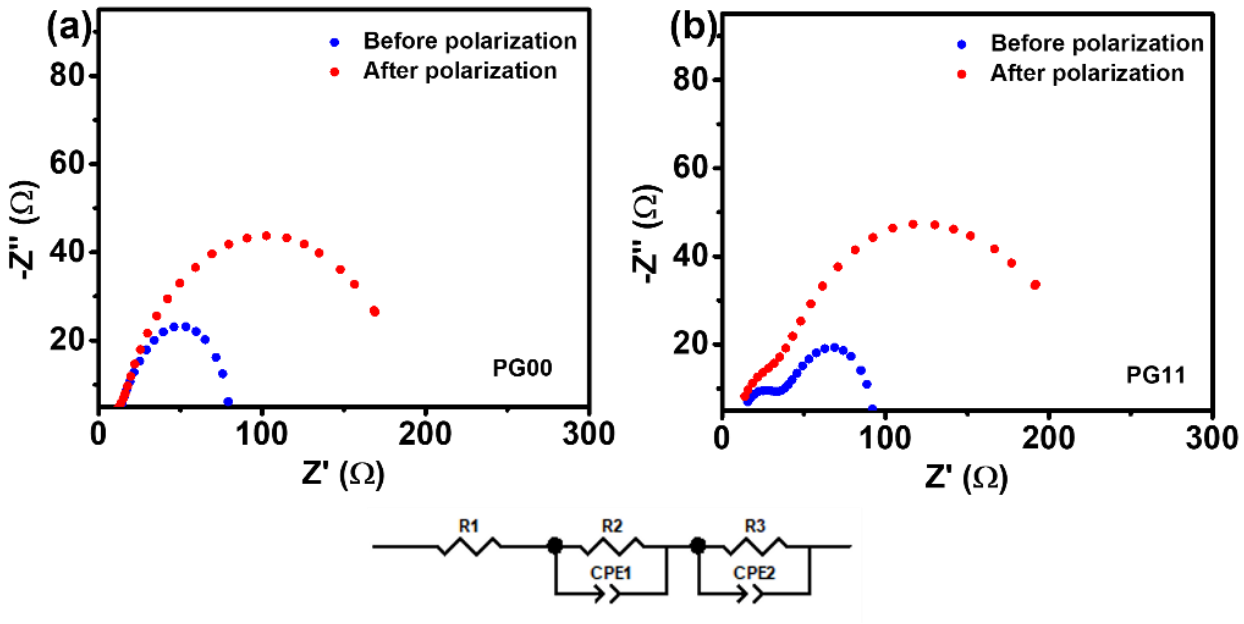

Figure S5. (a,b) Nyquist plots of the PG00 and PG11 GPEs recorded before and after DC polarization during the Zn^{2+} transference number measurements. The inset shows the equivalent circuit used for fitting the impedance spectra.

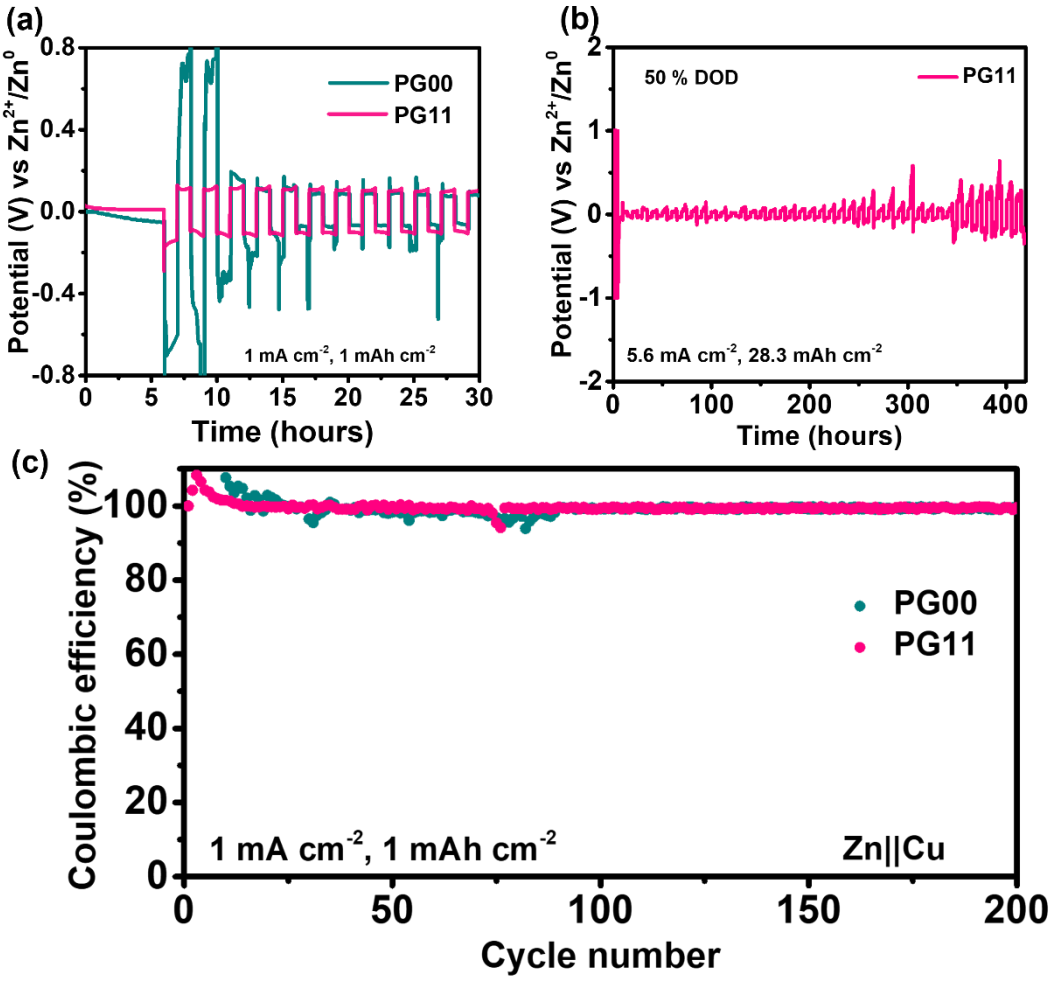

Figure S6. (a) Initial Zn plating/stripping profiles of Zn|Zn symmetric cells employing PG00 and PG11 at a current density of 1 mA cm^{-2} and an areal capacity of 1 mAh cm^{-2}; (b) Long-term Zn plating/stripping performance of the optimized PG11 electrolyte at 50% depth of discharge (DOD), corresponding to a current density of 5.6 mA cm^{-2} and an areal capacity of 28.3 mAh cm^{-2}; (c) Coulombic efficiency of Zn|Cu cells employing PG00 and PG11 during repeated Zn plating/stripping cycles at 1 mA cm^{-2} and 1 mAh cm^{-2}.

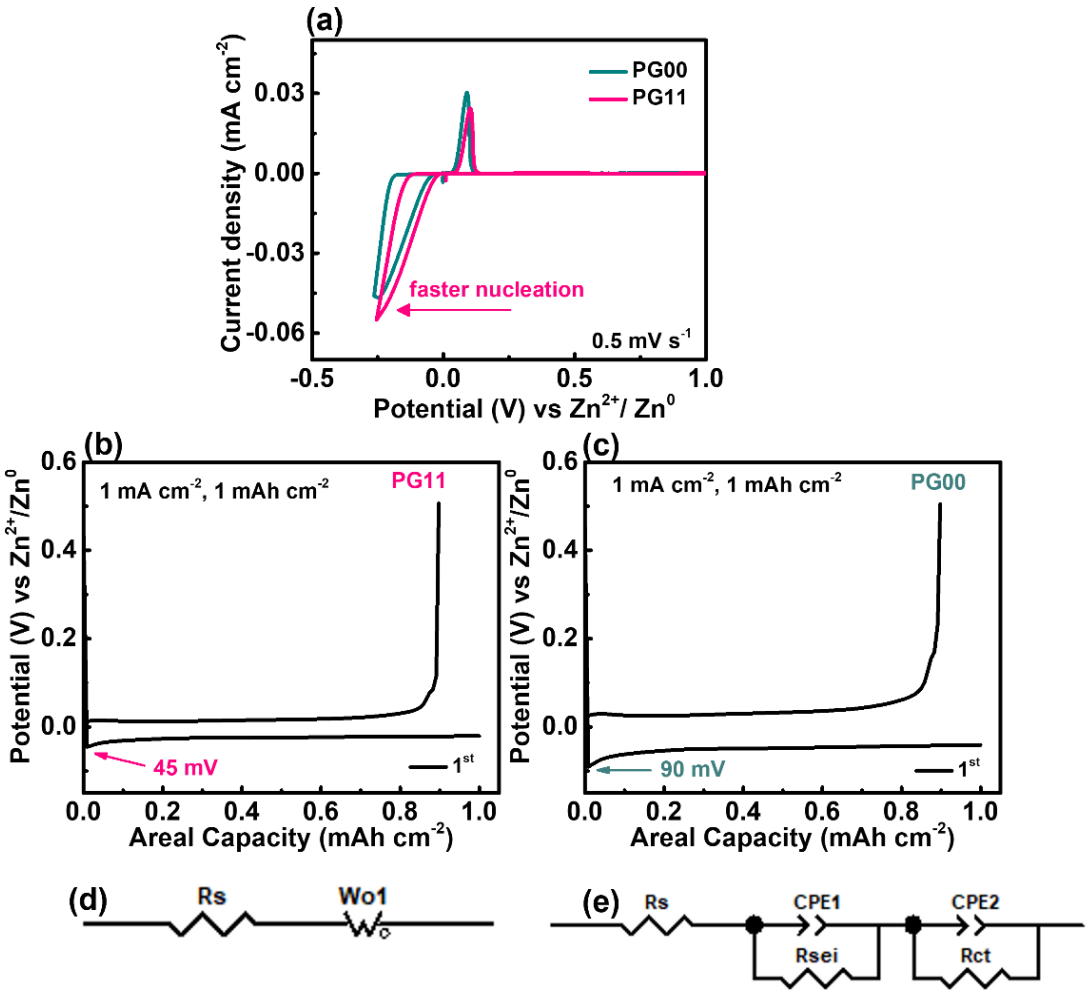

Figure S7. (a) Cyclic voltammograms of Zn|SS cells employing PG00 and PG11 at a scan rate of 0.5 mV s^{-1};. (b,c) Initial Zn nucleation overpotential of PG11 and PG00, respectively, determined from the first Zn plating cycle in Zn|Cu cells at 1 mA cm^{-2} and 1 mAh cm^{-2}; (d,e) Equivalent electrical circuits used for fitting the electrochemical impedance spectra measured at OCV and under the initial Zn nucleation bias, respectively.

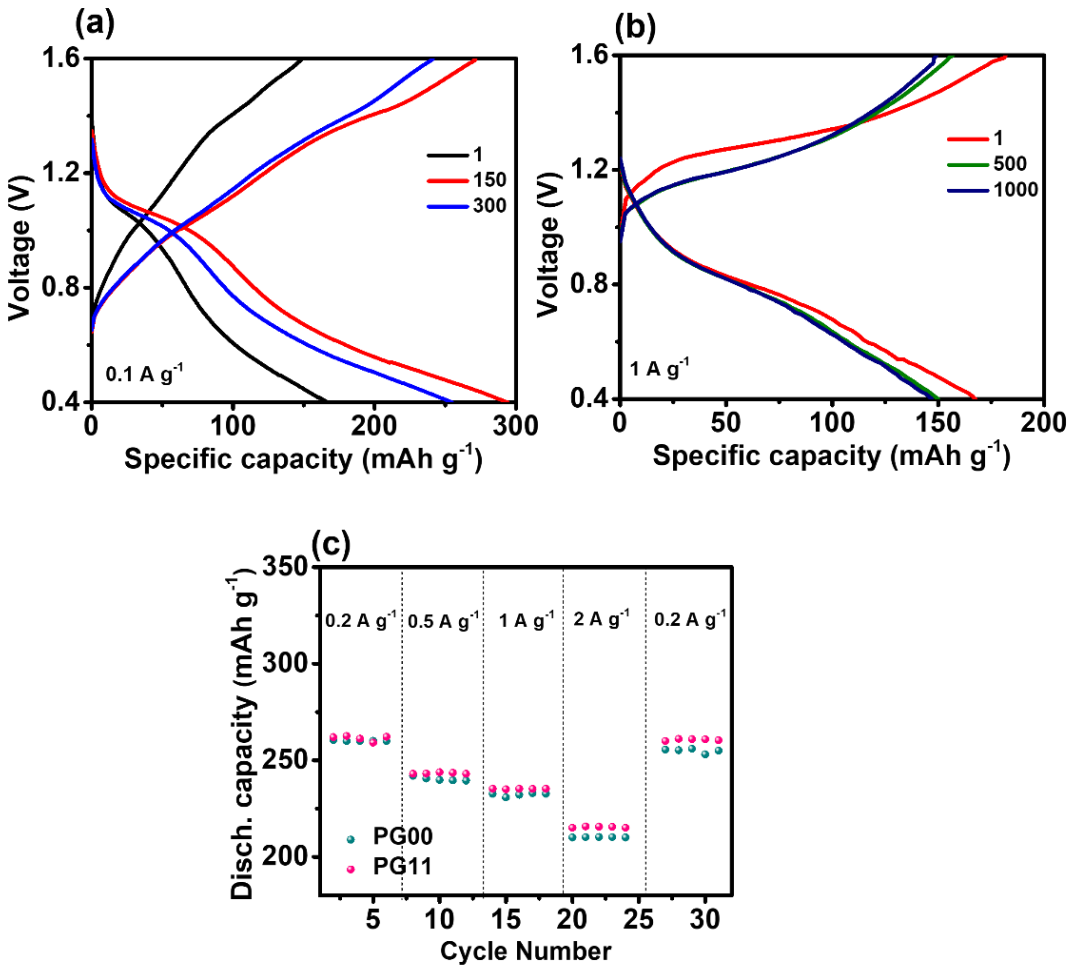

Figure S8. (a,b) Galvanostatic charge-discharge profiles of the Zn|V_2O_5 full cell employing the optimized PG11 GPE at 0.1 A g^{-1} and 1 A g^{-1}, respectively; (c) Rate performance comparison of Zn|V_2O_5 full cells employing PG00 and PG11 at current densities of 0.2, 0.5, 1, and 2 A g^{-1}, followed by recovery at 0.2 A g^{-1}.

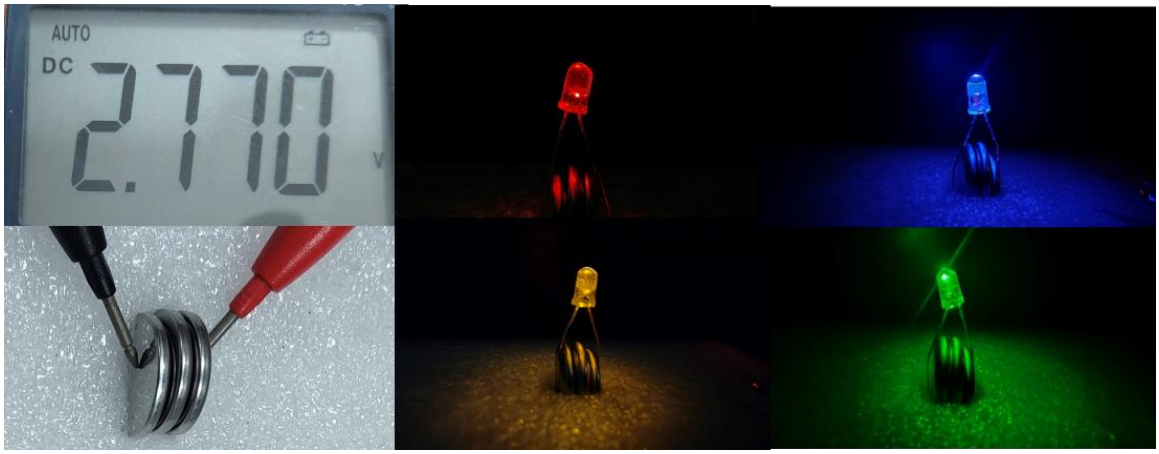

Figure S9. Demonstration of the practical applicability of the Zn|V_2O_5 full cells employing the optimized PG11 GPE. Three coin cells connected in series deliver an open-circuit voltage of 2.77 V and successfully power red, blue, yellow, and green light-emitting diodes (LEDs).

Table S1a. Bragg angle of the (200) reflection and calculated interchain spacing[1] of the GPE membranes.

Formulation	**Θ for (200) (°)**	**<R>=5/8 (λ/sinΘ) (Å)**
PG00	11.28	4.91
PG10	10.17	5.45
PG11	10.17	5.45
PG01	10.52	5.27

Table S1b. Percentage crystallinity[2,3] of the GPE membranes determined from XRD peak deconvolution.

Formulation	**Area under the curve of the crystalline peaks (A_C)**	**Total area under the curve (crystalline + amorphous) (A_t)**	**Percentage crystallinity (%) = A_c/A_t*100**
PG00	23.703	29.069	81.54
PG10	15.995	25.590	62.50
PG11	14.930	24.910	59.93
PG01	18.004	23.090	77.97

Table S2. Electrolyte uptake of the prepared GPE membranes after soaking in 3 M $ZnSO_4$ electrolyte.

Composition	**Initial weight (g)** (W_i)	**Final weight (g)** (W_a)	**Electrolyte uptake** **(%)**
PG00	0.062	0.109	76
PG10	0.072	0.150	109
PG11	0.069	0.188	172
PG01	0.069	0.150	143

Table S3. Ionic conductivity measurements of the prepared GPE membranes determined by EIS.

Membrane	**Thickness of wet membrane (cm)** (*l*)	**Bulk resistance (Ω)** (*R*)	**Ionic conductivity (mS cm^{-1})**
PG00	0.0216	11.02	1.10
PG10	0.0207	1.87	6.26
PG11	0.0249	1.90	7.33
PG01	0.0220	2.93	4.25

Contact area between electrodes and separator (A) = 1.766 cm^2

Table S4a. Relative viscosity of $ZnSO_4$ aqueous solutions at different concentrations.

Number of moles of $ZnSO_4$(M)	**Viscosity (η) (mPa sec)**	**Relative viscosity (η_r) = η/η_0**
0 (pure water)	203 (η_0)	1
1	272	1.33
2	383	1.88
3	434	2.13
4	572	2.81
5	715	3.52

Table S4b. Electrolyte uptake of the optimized PG11 GPE at different $ZnSO_4$ concentrations.

Concentration of $ZnSO_4$ (M)	**Initial weight (g) (W_i)**	**Final weight (g) (W_a)**	**Electrolyte uptake (%)**
1	0.068	0.269	297
2	0.065	0.195	201
3	0.056	0.155	178
4	0.063	0.128	104
5	0.061	0.095	56

Table S4c. Ionic conductivity measurements of the optimized PG11 GPE at different $ZnSO_4$ concentrations.

Concentration of $ZnSO_4$ (M)	**Thickness of wet membrane (cm) (*l*)**	**Bulk resistance (Ω) (*R*)**	**Ionic conductivity (mS cm^{-1})**
1	0.0280	3.24	4.89
2	0.0256	1.68	8.62
3	0.0248	1.55	9.06
4	0.0228	3.77	3.42
5	0.0210	6.11	1.94

Contact area between electrodes and separator (A) = 1.766 cm^2

Table S5. Zn^{2+} transference number of the prepared GPE membranes determined using the Bruce–Vincent method.

Membrane	**Initial current (mA) (I_o)**	**Steady-state current (mA) (I_s)**	**Initial resistance (Ω) (R_o)**	**Final resistance (Ω) (R_s)**	**t_{Zn2+}**
PG00	0.05	0.02	94	258	0.44
PG11	0.03	0.02	54	212	0.97

Step potential (ΔV) = 10 mV

Table S6. Fitted EIS parameters of PG00 and PG11 obtained under OCV and at the initial Zn nucleation bias.

Resistance type	**PG00**		**PG11**	
	OCV	**Bias**	**OCV**	**Bias**
R_s (Ω)	22.58	25.83	4.13	5.61
R_{SEI} (Ω)	-	159.5	-	86.99
R_{ct} (Ω)	-	305.4	-	90.67

Table S7. Literature comparison of plasticizer systems reported for zinc-based energy storage devices and the present dual-plasticizer GPE.

Polymer system	**Plasticizer**	**Salts**	**$\sigma_{r.t}$ (mS cm^{-1})**	**t_{Zn}^{2+}**	**Ref.**
PEGDGE (poly(ethylene glycol) diglycidyl ether)	Propylene carbonate (PC)	$Zn(OTf)_2$	0.377	-	[4]
Sodium alginate (SA)	Glycerol	$ZnSO_4$	32.8	-	[5]
Agar/PVA (polyvinyl alcohol)	Glycerol	$KOH+ZnCl_2$	125	0.67	[6]
P(SBMA/AM) (sulfobetaine-polyacrylamide)	Glycerol	$Zn(OTf)_2$	1.25 at -45 ˚C	-	[7]
PVdF-HFP (poly-(vinylidene fluoride-co-hexafluoropropylene))	Adiponitrile	$Zn(OTf)_2$	0.63	0.99	[8]
Poly(RM257)	Glycerol	$Zn(CH_3COO)_2$	0.0187	0.20	[9]
poly(vinyl chloride) (PVC)/poly(ethyl methacrylate) (PEMA)	EMIMTFSI (1-ethyl-3-methylimidazolium bis(trifluoromethylsulfonyl)imide)	$Zn(OTf)_2$	0.363	0.66	[10]

PDMAA (poly-(N,N-dimethylacrylamide))/PAM (polyacrylamide)	PC	$Zn(OTf)_2$	5.3	-	[11]
PEC (poly(ethylene carbonate))	Succinonitrile (SN)	$Zn(OTf)_2$	0.2392	0.61	[12]
Gelatin/SA	Glycerol	$ZnSO_4$	5.56	0.69	[13]
SA/PVA	Ethylene glycol	$ZnSO_4$	2.5	0.714	[14]
NaCMC	PC+Glycerol	$ZnSO_4$	9.06	0.97	This work

References

1. Dueramae, I., Okhawilai, M., Kasemsiri, P. & Uyama, H. High electrochemical and mechanical performance of zinc conducting-based gel polymer electrolytes. *Sci. Rep.* **11**, 1–15 (2021).

2. Adam, A. A. *et al.* Insight into the Effect of Glycerol on Dielectric Relaxation and Transport Properties of Potassium-Ion-Conducting Solid Biopolymer Electrolytes for Application in Solid-State Electrochemical Double-Layer Capacitor. *Molecules* **28**, (2023).

3. Dhanush, P. C. & Ismayil. Ionic transport and structural analysis of zinc chloride doped ί-carrageenan solid polymer electrolytes for energy storage devices. *J. Energy Storage* **145**, 119933 (2026).

4. Dong, H. *et al.* An anti-aging polymer electrolyte for flexible rechargeable zinc-ion batteries. *J. Mater. Chem. A* **8**, 22637–22644 (2020).

5. Shang, W. *et al.* Establishing High-Performance Quasi-Solid Zn/I2 Batteries with Alginate-Based Hydrogel Electrolytes. *ACS Appl. Mater. Interfaces* **13**, 24756–24764 (2021).

6. Zheng, Y. *et al.* Agar-assisted porous dual-network gel electrolyte: Boosting electrochemical performance of alkaline and neutral flexible zinc-air batteries. *Chem. Eng.*

J. **544**, 178797 (2026).

7. Zhang, Y. *et al.* Synergizing zwitterionic ion channels and hydrogen-bond reconfiguration for high-rate and low-temperature zinc-ion capacitors. *Chem. Eng. J.* **539**, 176922 (2026).

8. Kumar, A., Kumari, P., Parveen, S. & Hashmi, S. A. High Zn(II)-Ion Conduction via Ion–Solvent–Polymer Interactions in Gel Polymer Electrolyte with Adiponitrile Entrapped in Poly(vinylidene fluoride-co-hexafluoropropylene) and Application to Zinc-Ion Batteries. *ACS Appl. Energy Mater.* **9**, 4760–4775 (2026).

9. Prathumrat, P., Okhawilai, M., Likitaporn, C. & Uyama, H. Liquid crystalline elastomers/glycerol-based solid polymer electrolytes with shape memory properties for Zn-ion battery applications. *Mater. Res. Bull.* **181**, 113084 (2025).

10. Sai Prasanna, C. M. & Austin Suthanthiraraj, S. PVC/PEMA-based blended nanocomposite gel polymer electrolytes plasticized with room temperature ionic liquid and dispersed with nano-ZrO2 for zinc ion batteries. *Polym. Compos.* **40**, 3402–3411 (2019).

11. Chen, H. *et al.* Janus Gel Electrolyte Enabled High-Performance Quasi-Solid-State Electrochromic Zn-Ion Batteries. *ACS Appl. Polym. Mater.* **7**, 3718–3727 (2025).

12. Zhang, L. *et al.* A Poly(ethylene carbonate)-based all solid state zinc ion battery. *Electrochim. Acta* **470**, 143336 (2023).

13. Qian, D. *et al.* Green biomass-derived degradable hydrogel electrolytes for highly stable zinc-ion batteries. *Chem. Eng. J.* **537**, 176463 (2026).

14. Zhu, J. *et al.* Scalable Production of Motion-Enabled Self-Charging Power Textiles with Highly Durable Zinc-Ion Fiber Batteries. *Adv. Mater.* 1–15 (2026) doi:10.1002/adma.73836.